Limiting capabilities of two-dimensional plasmonics in electromagnetic wave detection

Dmitry Mylnikov and Dmitry Svintsov [*]

Laboratory of 2d Materials for Optoelectronics, Moscow Institute of Physics and Technology, Dolgoprudny 141700, Russia

Plasmons in two-dimensional electron systems (2DESs) feature ultrastrong confinement and are expected to efficiently mediate the interactions between light and charge carriers. Despite these expectations, the electromagnetic detectors exploiting 2D plasmon resonance have been so far inferior to their nonresonant counterparts. Here, we theoretically analyze the origin of these failures, and suggest a proper niche for 2D plasmonics in electromagnetic wave detection. We find that a confined 2DES supporting plasmon resonance has an upper limit of absorption cross section, which is identical to that of simple metallic dipole antenna. Small size of plasmonic resonators implies their weak dipole moments and impeded coupling to free-space radiation. Achieving the "dipole limit" of the absorption cross section in isolated 2DES is possible either at unrealistically long carrier momentum relaxation times, or at resonant frequencies below units of terahertz. We further show that amendment of even small metal contacts to 2DES promotes the coupling and reduces the fundamental mode frequency. The contacted resonators can still have deep-subwavelength size. They can be merged into compact arrays of detectors responding resonantly to multiple frequencies. Such arrays may find applications in multichannel wireless communications, hyper-spectral imaging, and energy harvesting.

I. INTRODUCTION

Two-dimensional plasmons represent a remarkable example of electromagnetic waves confined to scales 2 orders of magnitude below the free-space photon wavelength [1]. It is commonly articulated that confinement allows 2D plasmons to mediate strong light-matter interactions [2–4]. What is meant by this mediation remains largely unclear. The fundamental studies reveal intriguing properties of 2D plasmons [5–8], yet do not show a distinct promise for optoelectronics.

This long-reigning existential vacuum was filled by a proposal to use 2D plasmons for high-responsivity electromagnetic detection [9]. The idea partly followed the path of bulk plasmonics, with its established applications in photodetectors and solar cells [10]. More specifically, Ref. [9] suggested a confined 2D electron system (2DES) to act simultaneously as a resonant cavity and rectifier (detector) for 2D plasmons. The estimated detector response to free-space illumination scaled quadratically with plasmon quality factor, and promised sensitive detection for the practically useful terahertz range [11]. The idea ignited a booming research in the field of 2D plasmon-enhanced detectors, with further proposals based

on different materials [12–17], rectification mechanisms [18–22], and coupling schemes [23,24].

So far, the *experimentally realized* 2D plasmonic detectors [25–33] did not demonstrate substantial responsivity enhancement compared to their nonresonant counterparts [34–37]. Even if plasmonics was in play, and responsivity demonstrated clear maxima at plasmon frequencies [25,26,31,33], their height was not impressive for practical applications. Electronic quality of 2D systems and extra mechanisms of plasmon loss were typically blamed as limiting factors to the strength of plasmon resonance [27]. But even in the cleanest 2D systems with electron mobility exceeding millions of centimeters squared per volt per second, excitation of plasmons lead not to resonant enhancement of responsivity, but to responsivity oscillations [26,31].

These numerous experiments stimulate a critical reconsideration of advantages, which 2D plasmonics can bring to electromagnetic wave detection. In this paper, we show that plasmonic detectors based on confined 2DES possess a fundamental limit of electromagnetic absorption cross-section order of $\sigma_\lambda = \lambda_0^2/4\pi$, where λ_0 is the free-space wavelength [38]. This limit is identical for resonant plasmonic detectors and nonresonant structures matched to conventional antennas [39]; hence, a *single* plasmonic detector is not superior to the nonplasmonic one. Further, reaching this maximum cross section in plasmonic systems

---

is far more challenging, compared to antenna-coupled detectors. The reason is the small size of 2D plasmonic resonators, their small dipole moment, and weak coupling to free-space radiation.

We explore the ways to achieve perfect coupling between confined 2D plasmons and free-space radiation. We find that metal contacts, being an inevitable part of any photodetector, strongly modify the absorption cross section, matching conditions, and resonant frequencies. At fixed size of 2DES, the electron mobility which provides the best matching scales inversely proportionally to the contacts' length. For some contact geometries, the matching is achieved for surprisingly "dirty" electronic systems. Loosely speaking, a good plasmonic detector should have carefully engineered metal contacts, but not the highest-mobility 2D channel.

Despite the emerging identity between the responsivity of plasmonic and nonplasmonic detectors, we find a suitable niche for 2D plasmonic detectors. Exploiting the deep-subwavelength confinement, one can "pack" a large number of detectors even in the minimally focused light spot size of area approximately λ_0^2. Each detector can have an absorption cross section reaching σ_λ. Thus, the net signal collected from an array can largely exceed the signal from one nonplasmonic antenna-matched device (having a comparable area). Of note, the additive character of the cross section works if only plasmonic detectors within a spot are tuned to slightly different resonant frequencies. Applications of such detectors can lie in hyper-spectral imaging [40], multichannel wireless communication [41], and electromagnetic energy harvesting [42].

So far, the impedance-matching requirements for confined 2D plasmons have not yet been realized, though they received much attention in metal-insulator and nanoparticle plasmonics [43,44]. Recently, it was shown that short wavelength of *propagating* 2D plasmons implies their low excitation efficiency by small scatterers [45]. Interplay of Ohmic and radiative damping was recently studied for 2D plasmons in discs [46], but practically useful absorption cross sections were not analyzed. General constraints on extinction and absorption were recently derived in Ref. [47], but applications were demonstrated only for bulk plasmonic structures. The absorption cross sections limited by material loss in 2DES were analyzed in Ref. [48], but developed quasistatic theory did not reproduce the dipole cross-section limit.

Further on, we theoretically elucidate the strategies for making a plasmonic photodetector with a maximum radiation absorption cross section. We do not focus on a particular photocurrent generation mechanism (be it thermoelectric, bolometric, photovoltaic, or resistive self-mixing), as all of them are bounded by the absorbed power. The simulations are performed with the CST Microwave Studio package using the finite-element method, and supported by simple analytical estimates if possible.

II. ABSORPTION LIMITS BY CONFINED 2D PLASMONS

We start by examining the electromagnetic absorption by isolated two-dimensional systems without metal contacts [Fig. 1(a)]. This case, being not very practical for detectors, provides useful insights into matching conditions. The properties of 2DES are described in terms of kinetic inductance per square $L_\square$ and active resistance $R_\square$, such that sheet impedance $Z_\square = i\omega L_\square + R_\square$. The frequency dependence of Z can be arbitrary, and may originate from intra- and interband material processes; all we need in simulations is just the numerical value of Z at excitation frequency ω. If the conductivity is described by Drude model, $L_\square$ is linked to sheet carrier density n_s as $L_\square = m/n_s e^2$, and resistance $R_\square = m/n_s e^2 \tau$, where τ is the momentum relaxation time. The 2DES has a square shape with side g.

The calculated absorption spectrum of a square piece of 2DES ($g = 0.5~\mu$m) with kinetic inductance $L_\square = 20$ pH and moderate momentum relaxation time $\tau = 0.1$ ps is shown in Fig. 2. The parameters correspond to graphene with Fermi energy $E_F \approx 0.4$ eV and mobility $\mu = 2.4 \times 10^3$ cm^2/V s [49]. The plasmon resonance at $f_{res} \approx 15$ THz manifests as a clear absorption maximum, as the high-quality conditions are well fulfilled, $\omega_{res}\tau = 10 \gg 1$. The
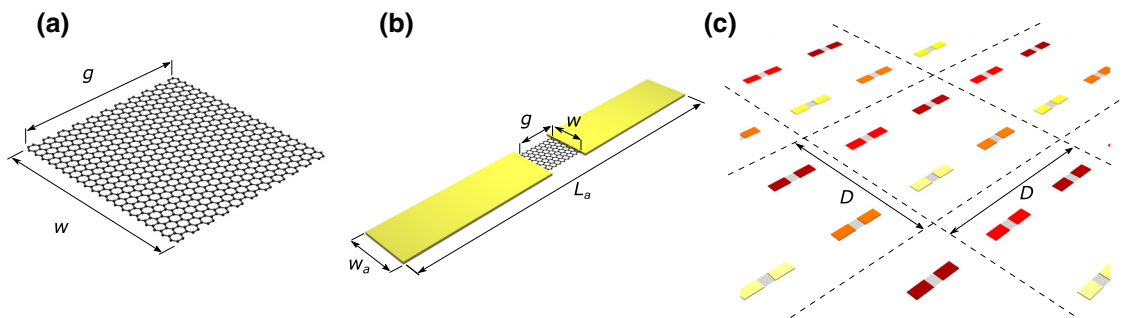

FIG. 1.   Two-dimensional plasmonic resonators. (a) Isolated layer of two-dimensional electronic system (graphene is shown as an example). (b) 2DES connected to metallic leads. (c) Multicolor array of plasmonic detectors.
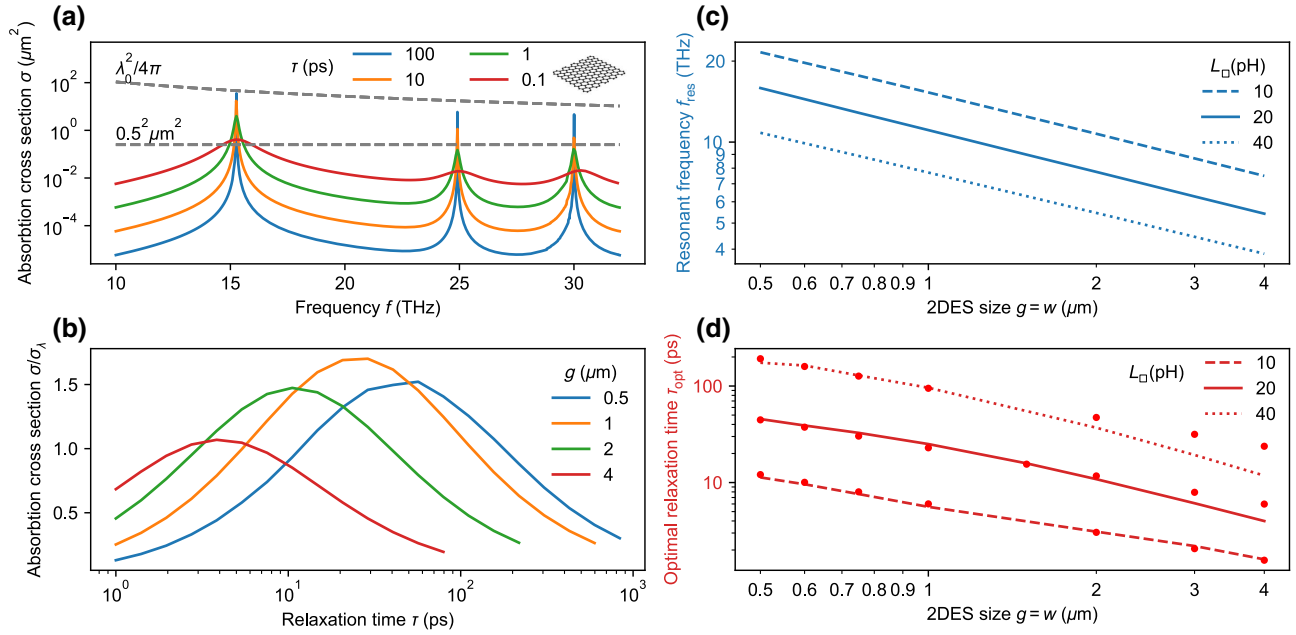
FIG. 2. Electromagnetic absorption by confined 2D plasmons. (a) Absorption cross-section spectrum of a square 2DES sheet ($g = w = 0.5$ μm) at different momentum relaxation times τ. Sheet inductance $L_\square = 20$ pH. (b) Absorption cross section at fundamental plasmonic resonance versus momentum relaxation time at variable size g: emergence of optimum momentum relaxation $\tau_{\rm opt}$. (c),(d) Dependence of resonant frequency $f_{\rm res}$ and matching time $\tau_{\rm opt}$ on 2DES size g for different values of sheet inductance $L_\square = 10, 20$, and 40 pH (controlled by carrier density). Dots in (d) are the results of numerical simulations, lines are calculated using analytical expression (1).

cross section largely exceeds the geometrical area of 2DES $\sigma \approx 10g^2$.

Would one obtain larger resonant absorption if the electronic quality of 2DES would be increased? We examine it by evaluating the cross sections for a sequence of relaxation times, $\tau = 1, 10$, and 100 ps. The resonant absorption $\sigma(f_{\rm res})$ initially grows, reaches a maximum at $\tau_{\rm opt} \approx 50$ ps, and then rolls down. The fundamental limits of cross section are best visualized if plotted in units of $\sigma_\lambda = \lambda_0^2/4\pi$ [Fig. 2(b)]. The cross section at optimum relaxation time is of the order of $3\sigma_\lambda/2$, which is a characteristic of dipole resonance limited by radiative decay [38].

The optimum relaxation time $\tau_{\rm opt} \sim 10 \cdots 100$ ps for reaching the best absorption at terahertz frequencies is quite large for realistic 2DES, as it corresponds to mobilities $\mu_{\rm opt} \approx (0.2 \cdots 2) \times 10^6$ cm^2/(V s). The very existence of optimum time hints that the resonant absorption maximum corresponds to some kind of matching. Further on, the optimum relaxation time becomes longer once the size of 2DES is decreased and its resonant frequency goes up. It suggests that the matching problem is associated with small size of plasmonic resonator, short wavelength of 2D plasmons, and ultimately weak radiation coupling of plasmonic systems.

To test this idea and get a simple estimate of optimum relaxation time, we equate the radiation losses $P_{\rm rad}$ and

Joule losses P_J in a piece of 2DES with high-frequency current distribution $\mathbf{j}_\omega(\mathbf{r})$ (Appendix A). This results in

$$\frac{4\pi}{3}\left(\frac{g}{\lambda_0}\right)^2 Z_0 \langle \mathbf{j}_\omega(\mathbf{r})\rangle^2 = 2R_\square \langle \mathbf{j}_\omega^2(\mathbf{r})\rangle, \tag{1}$$

where $Z_0 = 377$ Ω is the free-space impedance, and angular brackets $\langle\cdots\rangle$ denote averaging over the sample area. For a fundamental mode with nearly sinusoidal current distribution one can estimate $\langle \mathbf{j}_\omega^2(\mathbf{r})\rangle/\langle \mathbf{j}_\omega(\mathbf{r})\rangle^2 = \pi^2/8 \sim 1$. The inverse quadratic scaling of radiated power with wavelength is in agreement with recent experimental measurements [50].

The matching Eq. (1) has serious implications. The value of $\tau_{\rm opt}$ should be so large that Ohmic resistance $R_\square$ is $(\lambda_0/g)^2$ times smaller than free-space impedance. We note that sheet resistances below Z_0 were reached only recently in high-quality GaAs quantum wells [51], while typical graphene sheets have $R_\square \sim 1$ kOhm. The factor $(g/\lambda_0)^2$ requiring the smallness of Ohmic resistance is nothing but the measure of subwavelength compression achieved in a plasmonic resonator.

Scaling of optimum relaxation time with size of plasmon resonator g can be derived once the scaling of resonant frequency is known. As an estimate, one can "quantize" the dispersion of 2D plasmons in extended

system $\omega_{\mathrm{pl}}(q) = \sqrt{q/2\varepsilon_0 L_\square}$ at the characteristic wave vector $q = \pi/g$. As a result, $f_{\mathrm{res}} = (2\pi)^{-1}\omega_{\mathrm{pl}}(\pi/g)$ becomes inversely proportional to the square root of size, $f_{\mathrm{res}} \propto g^{-1/2}$, while optimum momentum relaxation time scales approximately as $1/g$. These trends are supported well by our numerical simulations demonstrated in Figs. 2(c) and 2(d).

The inverse scaling of matching time τ_{opt} with size of plasmonic structure g suggests that strong light absorption and high-responsivity detection may be achieved only at THz and sub-THz frequencies with very high quality of 2DES. Already for mid-infrared applications ($\lambda_0 \approx 3~\mu\mathrm{m}$), the matching time $\tau_{\mathrm{opt}} \sim 2$ ns exceeds the achievable values by 3 orders of magnitude. We further show that these severe matching conditions can be modified via engineering of metal contacts to 2DES.

III. MATCHING 2D PLASMONS TO FREE SPACE WITH METAL CONTACTS

Metal contacts are inevitably present in any semiconductor-based photodetector, and may affect the device electrodynamics. Previously, a strong effect of contacts on eigenmodes of 2D plasmons was demonstrated experimentally [52,53]. Here, we show that metal contacts of moderate length have a strong impact on radiative coupling of plasmonic devices, and considerably reduce τ_{opt}.

Figure 3 substantiates our suggestions by showing the spectrum of cross section (a), the resonant frequency, and optimum momentum relaxation time (d) for 2DES with finite-length metal arms. The first example shown in Fig. 3(a) shows that amendment of metal arms to square-shaped 2DES with moderate relaxation time
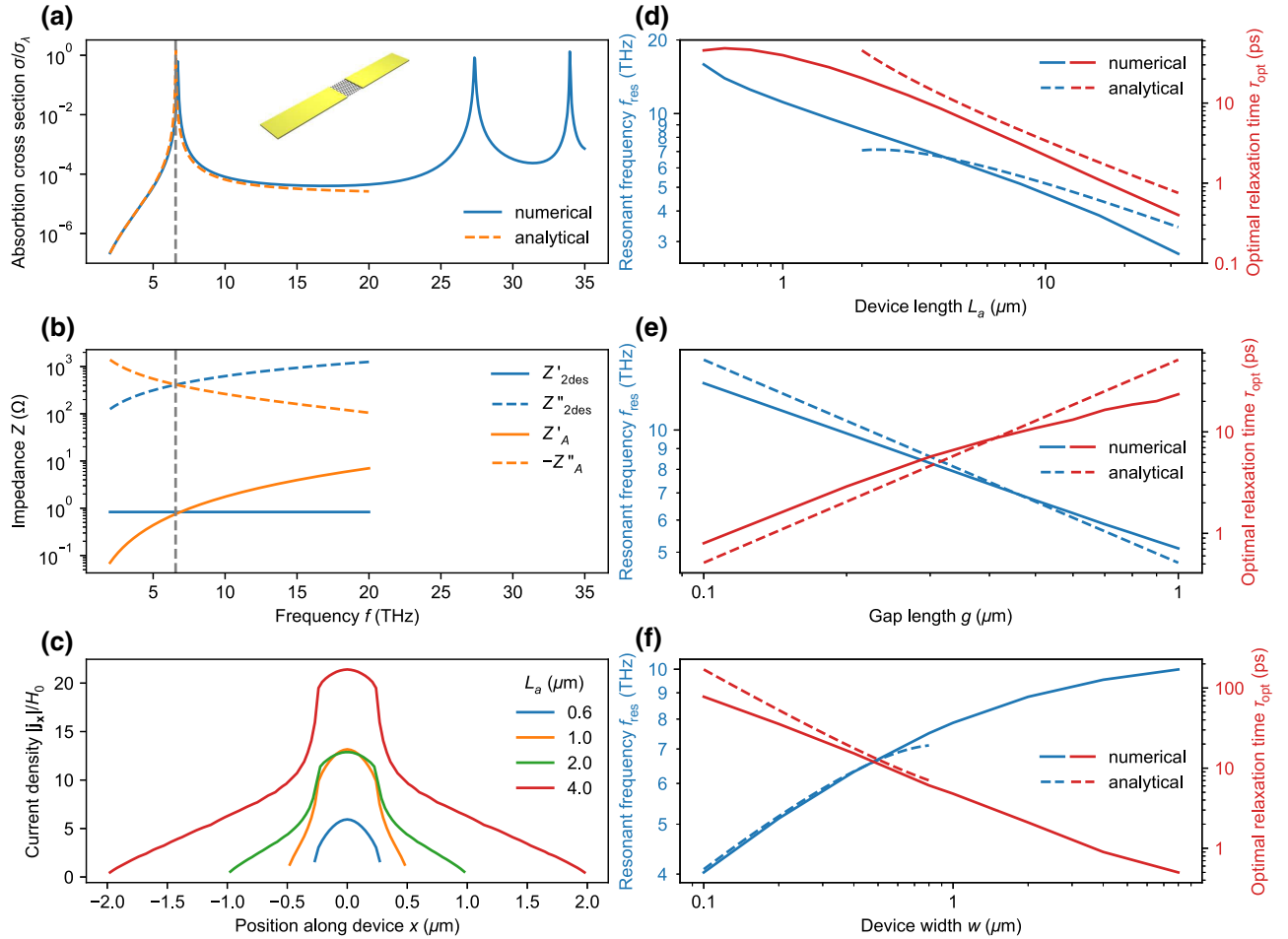

FIG. 3. Engineering the metal leads for coupling 2D plasmons to free-space radiation. (a) Absorption cross section of 2DES sheet of size $g = w = 0.5~\mu\mathrm{m}$ with metal arms. Total device length $L_a = 4~\mu\mathrm{m}$, width $w_a = w$, inductance $L_\square = 20$ pH, $\tau = \tau_{\mathrm{opt}} \approx 12$ ps. (b) Frequency scaling of 2DES (blue) and antenna (orange) impedance in the vicinity of fundamental resonance. (c) Distribution of induced currents $j_x(x, y = 0)$ along the contacted 2DES at resonance with increasing the length of metal arms. $\tau = 1$ ps. (d)–(f) Scaling of resonant frequency and optimum momentum relaxation time in contacted 2DES as functions of device length L_a (d), 2DES size g (e,) and device width $w = w_a$ (f).

$\tau = 12$ ps considerably enhances the cross section. Eventually, it can become close to the fundamental limit of σ_λ.

It is instructive to track the properties of fundamental plasmonic mode of 2DES with increase in device length L_a. Our simulations show that resonant frequency scales approximately as $f_{res} \propto L_a^{-1/2}$, while "matched" relaxation time scales as $\tau_{opt} \propto L_a^{-1}$ if the device length greatly exceeds the size of 2DES, $L_a \gg g$. Already for $L_a = 10$ μm and $g \approx 0.5$ μm, the optimum momentum relaxation time can take quite a realistic value ~ 3 ps. For the same contactless 2DES, the matched τ_{opt} is roughly an order of magnitude longer.

The above comparison of matching conditions in contacted and contactless 2DES is performed at given 2DES size. Of course, larger-area 2DESs also have shorter relaxation time, just as small 2DESs with large metal contacts. Comparing the values of τ_{opt} in contacted and contactless 2DES *at fixed resonant frequency*, we find them to be nearly identical. From the viewpoint of practical photodetection, it is desirable to use small 2DES with large metal arms, as this leads to enhancement of power density released in the 2D channel.

It is further possible to provide a simple model governing the matching of plasmonic resonators with the aid of contacts. A hint toward such a model lies in a very simple distribution of currents in contacted 2DES. While uncontacted 2DES at resonance has a nearly sinusoidal current distribution, this profile is quickly flattened toward constant value as L_a goes up [Fig. 3(c)]. It implies that effects of distributed inductance and capacitance are unimportant for contacted resonators, and simple lumped models can work well.

The desired lumped model is simply a series connection of 2DES with impedance $Z_{2Des} = (g/w)Z_\square$ and short metal dipole antenna with with impedance $Z_A = R_{rad} + (i\omega C_A)^{-1}$. Imaginary part of 2DES impedance is mainly due to kinetic inductance of 2D electrons. The impedance of short antenna ($l \ll \lambda_0$) is mainly governed by its capacitive gap. The resonant frequency in this case is simply given by [53]

$$\omega_0 = \frac{1}{\sqrt{L_\square C_A}} \sqrt{\frac{w}{g}}. \qquad (2)$$

To complete the model, we adopt the expressions for capacitance and radiative resistance of a short dipole antenna [39], $C_A \approx \pi/2\varepsilon_0 L_a \ln^{-1}[L_a/w_a - 1]$ and $R_{rad} = \pi/6Z_0(L_a/\lambda_0)^2$. The matching condition, in such a model, reads simply as $R_\square g/w = R_{rad}$, or, in extended form:

$$R_\square \frac{g}{w} = \frac{\pi}{6} Z_0 \left(\frac{L_a}{\lambda_0} \right)^2. \qquad (3)$$

The above analytical expressions confirm the numerically observed scaling of resonant frequency and matching

time, and correct them by a logarithmic factor $f_{res} \propto [L_a/\ln(L_a/w_a)]^{-1/2}$ and $\tau_{opt} \propto [L_a \ln(L_a/w_a)]^{-1}$. The lumped theory predicts the values of f_{res} and τ_{opt} very well, as seen from Figs. 3(d) and 3(e) by comparison of solid and dashed curves. Another option for increased matching of 2D plasmonic resonators lies in the increase of device width w. As soon as $w \ll \lambda_0$, increased width leads to quadratic enhancement of radiating dipole moment. This makes τ_{opt} drop abruptly as w increases, as shown in Fig. 3(f). Amending the antenna reciprocity theorem to the lumped model (Appendix B), one can further analytically predict the value of σ, as demonstrated in Fig. 3 with the dashed line.

IV. POSSIBLE NICHES FOR 2D PLASMONIC DEVICES

We demonstrate that upper bounds for the absorption cross section are identical for the 2D plasmonic structures and classical dipole-type antennas. It implies that plasmonic resonance in 2DES cannot help increasing the responsivity, compared to an optimally matched nonplasmonic device. This contrasts to numerous previous expectations [9,21,22], which did not properly consider the impedance matching for 2D plasmonic structures.

Of course, a plasmonic detector occupies ultrasmall area, and it is tempting to see whether small area may have practical consequences. Indeed, the size of optimally matched contacted structures considered in Fig. 3 did not exceed 0.5×4 μm^2 for resonant frequency of approximately 7 THz. It implies that the device area is just 0.1% of λ_0^2. All the saved space on a chip can be occupied with analog or digital electronic devices for signal processing. This is a purely economic (yet useful) benefit. One may wonder whether it is possible to use the remaining space for accommodating similar plasmonic detectors, and to increase the photovoltage and photocurrent by their serial and parallel connection. We address this problem in Sec. IV A.

For smaller resonant frequencies—say, approximately 100 GHz considered as a frontier for future wireless and mobile communications—2D plasmonics is the only solution for making on-chip antennas. This contrasts to current external antennas used in the smartphones. 2D plasmonic detectors are continuously tunable by the gate voltage, which contrasts to current tunable antennas using electrically switchable connections to the conducting arms of different length [54]. Further in Sec. IV B, we show that even a moderate-mobility 2DES with antenna pads can demonstrate wide tuning of the resonant frequency via changing the carrier density.

A. Plasmonic antenna arrays for multichannel communications

While a single 2D plasmonic resonator and an optimally loaded dipole antenna have the same absorption

cross sections, it may be tempting to exploit the small size of plasmonic cavities for the design of detector arrays [Fig. 1(c)]. By connecting the devices in series (or in parallel), one may progressively increase the photovoltage (or photocurrent) generated by such an assembly. One can estimate the maximum number of plasmonic devices per optimally focused light spot as $N \sim (\lambda_0 / \lambda_{pl})^2$. Thus, one may expect an N-fold enhancement of plasmonic metadevice responsivity, compared to a nonplasmonic device using classical antenna focusing.

Such packing is hardly possible if all detectors are tuned to the same resonant frequency. The emerging complexities for plasmonic arrays are illustrated in Fig. 4. Here, we plot the absorbance $\alpha(f)$ by a square-lattice array of plasmonic detectors tuned to $f_0 \sim 13$ THz versus the lattice period D. The absorbance is defined as the cross section per unit cell area, $\alpha = \sigma / D^2$. As the packaging becomes denser, the absorbance first goes up ($D \lesssim 10 \ \mu$m). By further increasing the density, we observe a strong degradation of α. Instructively, the optimal cell period appears

to be order of $(3\sigma_\lambda / 2)^{1/2} \approx 8 \ \mu$m. It implies that the plasmonic device at a resonance strongly distorts the field in a large nearby area approximately σ_λ, and exploiting the "compactness" advantage of plasmonics becomes impossible for single-frequency detection. Thus, the "effectively occupied area" by plasmonic cavity is still order of σ_λ, and hence order of size of a classical antenna.

The situation becomes more encouraging once we recall that large absorption cross section occurs only at the resonant frequency. One may thus use the σ_λ circle near the 2D plasmonic detector for placing other detectors tuned to different frequencies. Dissimilar devices do not hinder each other's absorption, provided their line width $\delta\omega \sim \tau^{-1} + \tau_{opt}^{-1}$ exceeds the spacing between resonant frequencies. Figure 4(b) substantiates this idea and compares the absorbance of single-color array (orange line) with that of four-color array of the same period (blue line). Although formal lattice periods for these arrays are equal, the area per element in the multicolor case is 4 times smaller. Each of four tuned devices fully exploits its resonant cross section.

We may suggest three application domains for such detector arrays. First of all, they can be exploited for sensitive detection of signals comprised of several wavelengths. This situation is common for multichannel wireless communications. The plasmonic detector array resonantly responding to all M communication wavelengths occupies the space $\lesssim \sigma_\lambda$. Achieving the same result with classical dipole antennas would require the area of $M\sigma_\lambda$, which becomes highly impractical for $M \gg 1$. Another currently used option for multichannel communications is based on broadband antennas with subsequent notch filters [55]. 2D plasmonic arrays responding to multiple wavelengths offer a much simpler option due to the presence of complex filtering structures. When dealing with multifrequency plasmonic arrays, individual devices should be contacted independently to reduce the total resistance and reduce the noise-equivalent power.

Second, the arrays of plasmonic detectors connected in series can effectively generate photovoltage upon illumination by broadband signals. The limiting example of such broadband signal is the background radiation noise, nowadays considered as a source for energy harvesting. Finally, plasmonic arrays can find applications for compact hyperspectral imagers, where the signal from each resonating element is proportional to the light intensity at a given frequency.
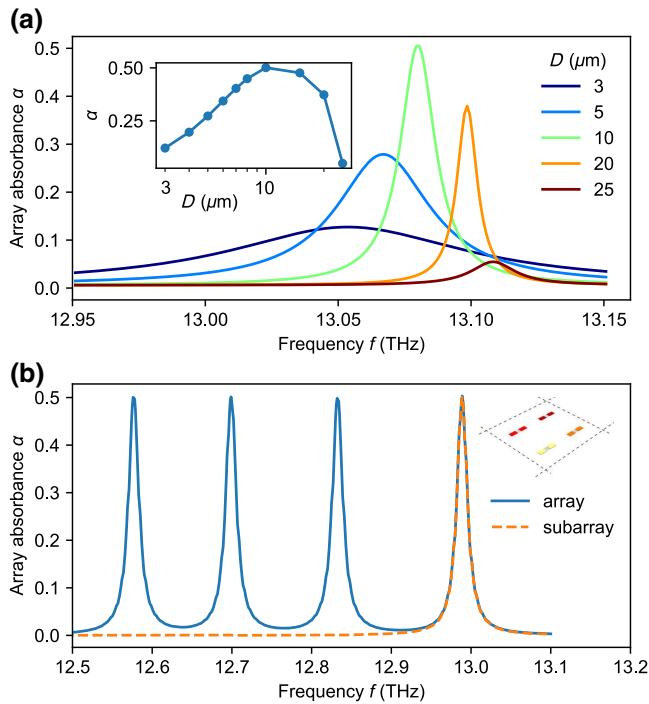
FIG. 4. Single and multicolor arrays of plasmonic photodetectors. (a) Absorbance spectrum $\alpha(f)$ of a single-color array, i.e., a square-lattice of identical plasmonic detectors. Different lines correspond to different cell periods D. Inset: resonant absorbance versus period. (b) Absorption spectrum of the four-color array with optimum cell period $D = 10 \ \mu$m. The absorbances of individual detectors are noninterfering and each reaches a maximum value of 0.5. Inductance $L_\square = 20$ pH, 2DES lengths $g = 300, 310, 320, 330$ nm, width $w = w_a = 500$ nm, total length $L_a = 1 \ \mu$m, $\tau = \tau_{opt} = 23$ ps.

B. Tunable resonant detectors and spectrometers with moderate-mobility 2DES

Another key advantage of 2D plasmonic resonators, apart from deep-subwavelength size, is the tuning of eigenfrequency upon variations of sheet conductivity Z_{2DES}. The latter is enabled *in situ* by electric field effect or transverse
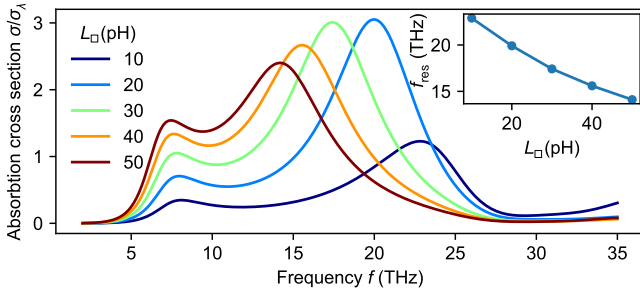
FIG. 5. Resonant and tunable absorption by low-mobility 2DES. Calculated spectrum of absorption cross section for small ($g = 0.1$ μm) moderate-quality 2DES ($\tau = 50$ fs) coupled to large antenna $L_a = 16$ μm, $w = w_a = 8$ μm. The highest peak occurs at frequency where $\lambda_0 \sim L_a$.

magnetic field. Frequency tuning enables the realization of all-electrical plasmonic radiation spectrometers. The deep confinement for such devices is unimportant, while a large absorption cross section is still highly desirable.

We show that a functional all-electric spectrometer (or tunable resonant detector) can be realized with "dirty" 2D electron systems and resonant metal antennas with size approximately λ_0. Figure 5 substantiates our findings by showing the absorption spectrum of 2DES-loaded antenna ($L_a = 16$ μm, $w_a = 8$ μm) at various 2D inductances. Instructively, the cross section at the second resonance reaches $(1 \cdots 3)\sigma_\lambda$, while the momentum relaxation time is moderate, $\tau = 50$ fs. The resonant frequency goes down with increasing $L_\square$ (inset), as it typically occurs in plasmonic systems.

The origin of large cross section and wide frequency tuning in this example come from the special design of arms having the length order of λ_0. Electric current has a node in the middle of the structure, and reaches large values in the metal arms. This enables matching of high-impedance structures to free space. On the other hand, bare antenna impedance strongly varies with frequency once its length is close to λ_0, and small variations of load impedance can lead to pronounced variations of the net resonant frequency.

V. DISCUSSION AND CONCLUSIONS

The presented study aims to indicate a possible niche for 2D plasmonics in photodetection applications. We try to dispel a common view that a high-quality factor for 2D plasmons is a necessary and sufficient condition for making a good plasmonic photodetector. Instead, we show that a good plasmonic photodetector requires impedance matching between radiative and Ohmic resistances. This is most simply achieved by engineering metal contacts to 2DES. In some situations (like at the midinfrared frequencies), large electron momentum relaxation time is indeed

essential. The quality requirements to 2DES are, however, becoming less relevant for THz and sub-THz frequencies.

In our study, we omit the consideration of photodetectors based on grating-coupled 2DES [23,24,28], but we expect the matching requirements similar to Eq. (1) to appear in that case. An approximate theory for absorption by such gratings [56] indeed points to the existence of such matching, but is applicable only to weakly coupled grating and 2DES. We also have not considered the 2D photodetectors with arrays of plasmonic particles for enhanced absorption [57,58], as they belong to the field of metal plasmonics and have no relation to 2D plasmonics.

It is tempting to reveal why previous proposals of the resonant plasmonic detectors [9,16–18,22] strongly overestimated their responsivities. The reason lies in the assumption that incident electromagnetic field can be mapped to a perfect voltage source with zero internal resistance. Assuming very long momentum relaxation time, one could obtain arbitrarily large Q factor of plasmon resonance. In reality, radiative resistance R_{rad} of all plasmonic systems is finite. Moreover, radiative resistance is linked to the ability of detector to receive power from free space. By releasing the assumption of voltage source ideality, one immediately realizes the existence of limiting responsivity for plasmonic radiation detectors.

VI. ACKNOWLEDGMENTS

APPENDIX A: MATCHING THE ABSORBED AND RADIATED POWER

We derive the matching condition by equating the absorbed (P_{abs}) and radiated (P_{rad}) powers in confined 2DES with current distribution $\mathbf{j}_\omega(\mathbf{r})$. We start with power radiated by a small dipole,

$$P_{\text{rad}} = Z_0 \frac{\omega^4}{3\pi c^2} |\mathbf{d}_\omega|^2. \tag{A1}$$

We re-express the dipole moment via current distribution using its definition, $\mathbf{d}_\omega = \int \mathbf{r}\rho_\omega(\mathbf{r})d^2\mathbf{r}$, and continuity equation $-i\omega\rho_\omega + \partial_{\mathbf{r}}\mathbf{j} = 0$. This results in

$$\mathbf{d}_\omega = \frac{1}{i\omega} \int \mathbf{j}_\omega(\mathbf{r})d\mathbf{r}. \tag{A2}$$

Introducing Eq. (A2) into Eq. (A1), and expressing the frequency via wavelength, $\omega = 2\pi c/\lambda_0$, we find

$$P_{\text{rad}} = Z_0 \frac{4\pi}{3\lambda_0^2} \left| \int \mathbf{j}_\omega(\mathbf{r})d\mathbf{r} \right|^2, \tag{A3}$$

which is equivalent to the left-hand side of Eq. (1) of the main text. As for absorbed power, it is simply given by

Joule's law:

$$P_{\text{abs}} = 2\text{Re}[Z_{\text{2DES}}(\omega)] \int |\mathbf{j}_\omega(\mathbf{r})|^2 d\mathbf{r}. \qquad \text{(A4)}$$

For the Drude model of conductivity, $\text{Re}[Z_{\text{2DES}}(\omega)]$ is nothing but dc sheet resistance $R_\square$. This brings us exactly to Eq. (1) of the main text.

APPENDIX B: ANALYTICAL MODEL FOR ABSORPTION OF CONTACTED 2D PLASMONIC DEVICE

The developed model for resonant frequencies and matching conditions can be further extended to fully analytical estimates of absorption cross section. It is based on the reciprocity theorem for antennas [39], and enables a cross section of contacted plasmonic resonator to be presented as

$$\sigma = \frac{\lambda_0^2}{4\pi} e_{\text{match}} D(\theta, \phi), \qquad \text{(B1)}$$

where $D(\theta, \phi)$ is the antenna directivity and

$$e_{\text{match}} = \frac{4 R_{\text{rad}} R_{\text{2DES}}}{|Z_A + Z_{\text{2DES}}^*|^2} \qquad \text{(B2)}$$

is the matching efficiency, which turns to unity for a perfectly matched device. For dipole radiation, which is always the case for the fundamental mode of subwavelength plasmonic resonator, $D(\theta, \phi) = 3/2 \sin^2 \theta$, and θ is the angle between dipole direction and wave vector of incident (radiated) light. We observe that the antenna model for cross sections works very well for prediction of absorption cross sections, as seen from comparison of dashed and solid lines in Fig. 3(a).

[1] F. Stern, Polarizability of a Two-Dimensional Electron Gas, Phys. Rev. Lett. **18**, 546 (1967).

[2] F. H. Koppens, D. E. Chang, and F. J. García De Abajo, Graphene plasmonics: A platform for strong light-matter interactions, Nano Lett. **11**, 3370 (2011).

[3] A. N. Grigorenko, M. Polini, and K. S. Novoselov, Graphene plasmonics, Nat. Photon. **6**, 749 (2012).

[4] F. J. García de Abajo, Graphene plasmonics: Challenges and opportunities, ACS Photonics **1**, 135 (2014).

[5] G. X. Ni, A. S. McLeod, Z. Sun, L. Wang, L. Xiong, K. W. Post, S. S. Sunku, B.-Y. Jiang, J. Hone, C. R. Dean, M. M. Fogler, and D. N. Basov, Fundamental limits to graphene plasmonics, Nature **557**, 530 (2018).

[6] A. Woessner, M. B. Lundeberg, Y. Gao, A. Principi, P. Alonso-González, M. Carrega, K. Watanabe, T. Taniguchi, G. Vignale, M. Polini, J. Hone, R. Hillenbrand, and F. H. L. Koppens, Highly confined low-loss plasmons in graphene–boron nitride heterostructures, Nat. Mater. **14**, 421 (2015).

[7] G. Scalari, C. Maissen, D. Turcinkova, D. Hagenmuller, S. De Liberato, C. Ciuti, C. Reichl, D. Schuh, W. Wegscheider, M. Beck, and J. Faist, Ultrastrong coupling of the cyclotron transition of a 2D electron gas to a THz metamaterial, Science **335**, 1323 (2012).

[8] P. Alonso-Gonzalez, A. Y. Nikitin, F. Golmar, A. Centeno, A. Pesquera, S. Velez, J. Chen, G. Navickaite, F. Koppens, A. Zurutuza, F. Casanova, L. E. Hueso, and R. Hillenbrand, Controlling graphene plasmons with resonant metal antennas and spatial conductivity patterns, Science **344**, 1369 (2014).

[9] M. Dyakonov and M. Shur, Detection, mixing, and frequency multiplication of terahertz radiation by two-dimensional electronic fluid, IEEE Trans. Electron Devices **43**, 380 (1996).

[10] H. A. Atwater and A. Polman, Plasmonics for improved photovoltaic devices, Nat. Mater. **9**, 865 (2010).

[11] K. Sengupta, T. Nagatsuma, and D. M. Mittleman, Terahertz integrated electronic and hybrid electronic–photonic systems, Nat. Electron. **1**, 622 (2018).

[12] A. Tredicucci and M. S. Vitiello, Device concepts for graphene-based terahertz photonics, IEEE J. Sel. Top. Quantum Electron. **20**, 130 (2014).

[13] L. Viti, D. Coquillat, A. Politano, K. A. Kokh, Z. S. Aliev, M. B. Babanly, O. E. Tereshchenko, W. Knap, E. V. Chulkov, and M. S. Vitiello, Plasma-wave terahertz detection mediated by topological insulators surface states, Nano Lett. **16**, 80 (2016).

[14] L. Viti, J. Hu, D. Coquillat, W. Knap, A. Tredicucci, A. Politano, and M. S. Vitiello, Black phosphorus terahertz photodetectors, Adv. Mater. **27**, 5567 (2015).

[15] D. Yavorskiy, M. Szoła, K. Karpierz, R. Bożek, R. Rudniewski, G. Karczewski, T. Wojtowicz, J. Wróbel, and J. Łusakowski, Grating metamaterials based on CdTe/CdMgTe quantum wells as terahertz detectors for high magnetic field applications, Appl. Sci. **10**, 2807 (2020).

[16] A. Tomadin and M. Polini, Theory of the plasma-wave photoresponse of a gated graphene sheet, Phys. Rev. B **88**, 205426 (2013).

[17] B. Winstanley, H. Schomerus, and A. Principi, Corbino field-effect transistors in a magnetic field: Highly tunable photodetectors, Phys. Rev. B **104**, 165406 (2021).

[18] V. Ryzhii and M. S. Shur, Resonant terahertz detector utilizing plasma oscillations in two-dimensional electron system with lateral schottky junction, Jpn. J. Appl. Phys. **45**, L1118 (2006).

[19] V. V. Popov, Terahertz rectification by periodic two-dimensional electron plasma, Appl. Phys. Lett. **102**, 253504 (2013).

[20] A. Principi, D. Bandurin, H. Rostami, and M. Polini, Pseudo-euler equations from nonlinear optics: Plasmon-assisted photodetection beyond hydrodynamics, Phys. Rev. B **99**, 075410 (2019).

[21] V. Y. Kachorovskii, S. L. Rumyantsev, W. Knap, and M. Shur, Performance limits for field effect transistors as terahertz detectors, Appl. Phys. Lett. **102**, 223505 (2013).

[22] M. Ryzhii, V. Ryzhii, T. Otsuji, V. Mitin, and M. S. Shur, Coulomb drag and plasmonic effects in graphene

field-effect transistors enable resonant terahertz detection, Appl. Phys. Lett. **120,** 111102 (2022).

[23] P. Olbrich, J. Kamann, M. König, J. Munzert, L. Tutsch, J. Eroms, D. Weiss, M.-H. Liu, L. E. Golub, E. L. Ivchenko, V. V. Popov, D. V. Fateev, K. V. Mashinsky, F. Fromm, T. Seyller, and S. D. Ganichev, Terahertz ratchet effects in graphene with a lateral superlattice, Phys. Rev. B **93,** 075422 (2016).

[24] J. A. Delgado-Notario, V. Clericò, E. Diez, J. E. Velázquez-Pérez, T. Taniguchi, K. Watanabe, T. Otsuji, and Y. M. Meziani, Asymmetric dual-grating gates graphene FET for detection of terahertz radiations, APL Photon. **5,** 066102 (2020).

[25] P. S. Dorozhkin, S. V. Tovstonog, S. A. Mikhailov, I. V. Kukushkin, J. H. Smet, K. Von Klitzing, K. V. Klitzing, and K. Von Klitzing, Resonant detection of microwave radiation in a circular two-dimensional electron system with quantum point contacts, Appl. Phys. Lett. **87,** 5 (2005).

[26] V. M. Muravev and I. V. Kukushkin, Plasmonic detector/spectrometer of subterahertz radiation based on two-dimensional electron system with embedded defect, Appl. Phys. Lett. **100,** 10 (2012).

[27] W. Knap, Y. Deng, S. Rumyantsev, J.-Q. Lü, M. S. Shur, C. A. Saylor, and L. C. Brunel, Resonant detection of subterahertz radiation by plasma waves in a submicron field-effect transistor, Appl. Phys. Lett. **80,** 3433 (2002).

[28] X. G. Peralta, S. J. Allen, M. C. Wanke, N. E. Harff, J. A. Simmons, M. P. Lilly, J. L. Reno, P. J. Burke, and J. P. Eisenstein, Terahertz photoconductivity and plasmon modes in double-quantum-well field-effect transistors, Appl. Phys. Lett. **81,** 1627 (2002).

[29] X. Cai, A. B. Sushkov, M. M. Jadidi, L. O. Nyakiti, R. L. Myers-Ward, D. K. Gaskill, T. E. Murphy, M. S. Fuhrer, and H. D. Drew, Plasmon-enhanced terahertz photodetection in graphene, Nano Lett. **15,** 4295 (2015).

[30] M. Freitag, T. Low, W. Zhu, H. Yan, F. Xia, and P. Avouris, Photocurrent in graphene harnessed by tunable intrinsic plasmons, Nat. Commun. **4,** 1951 (2013).

[31] V. M. Muravev, A. A. Fortunatov, A. Dremin, and I. V. Kukushkin, Plasmonic interferometer for spectroscopy of microwave radiation, JETP. Lett. **103,** 380 (2016).

[32] J. D. Chudow, D. F. Santavicca, and D. E. Prober, Terahertz spectroscopy of individual single-walled carbon nanotubes as a probe of Luttinger liquid physics, Nano Lett. **16,** 4909 (2016).

[33] D. A. Bandurin, D. Svintsov, I. Gayduchenko, S. G. Xu, A. Principi, M. Moskotin, I. Tretyakov, D. Yagodkin, S. Zhukov, T. Taniguchi, K. Watanabe, I. V. Grigorieva, M. Polini, G. N. Goltsman, A. K. Geim, and G. Fedorov, Resonant terahertz detection using graphene plasmons, Nat. Commun. **9,** 5392 (2018).

[34] S. Castilla, B. Terrés, M. Autore, L. Viti, J. Li, A. Y. Nikitin, I. Vangelidis, K. Watanabe, T. Taniguchi, E. Lidorikis, M. S. Vitiello, R. Hillenbrand, K. J. Tielrooij, and F. H. Koppens, Fast and sensitive terahertz detection using an antenna-integrated graphene pn junction, Nano Lett. **19,** 2765 (2019).

[35] L. Viti, D. G. Purdie, A. Lombardo, A. C. Ferrari, and M. S. Vitiello, Hbn-encapsulated, graphene-based,

room-temperature terahertz receivers, with high speed and low noise, Nano Lett. **20,** 3169 (2020).

[36] I. Gayduchenko, S. G. Xu, G. Alymov, M. Moskotin, I. Tretyakov, T. Taniguchi, K. Watanabe, G. Goltsman, A. K. Geim, G. Fedorov, D. Svintsov, and D. A. Bandurin, Tunnel field-effect transistors for sensitive terahertz detection, Nat. Commun. **12,** 543 (2021).

[37] M. Bauer, A. Ramer, S. A. Chevtchenko, K. Y. Osipov, D. Cibiraite, S. Pralgauskaite, K. Ikamas, A. Lisauskas, W. Heinrich, V. Krozer, and H. G. Roskos, A high-sensitivity AlGaN/GaN HEMT terahertz detector with integrated broadband bow-tie antenna, IEEE Trans. Terahertz Sci. Technol. **9,** 430 (2019).

[38] S. Tretyakov, Maximizing absorption and scattering by dipole particles, Plasmonics **9,** 935 (2014).

[39] C. A. Balanis, *Antenna Theory: Analysis and Design* (John wiley & sons, Hoboken (New Jersey), 2015).

[40] F. Yesilkoy, E. R. Arvelo, Y. Jahani, M. Liu, A. Tittl, V. Cevher, Y. Kivshar, and H. Altug, Ultrasensitive hyperspectral imaging and biodetection enabled by dielectric metasurfaces, Nat. Photonics **13,** 390 (2019).

[41] T. Nagatsuma, G. Ducournau, and C. C. Renaud, Advances in terahertz communications accelerated by photonics, Nat. Photon. **10,** 371 (2016).

[42] A. Sharma, V. Singh, T. L. Bougher, and B. A. Cola, A carbon nanotube optical rectenna, Nat. Nanotechnol. **10,** 1027 (2015).

[43] P. Spinelli, M. Hebbink, R. de Waele, L. Black, F. Lenzmann, and A. Polman, Optical impedance matching using coupled plasmonic nanoparticle arrays, Nano Lett. **11,** 1760 (2011).

[44] P. Ginzburg and M. Orenstein, Plasmonic transmission lines: from micro to nano scale with $\lambda/4$ impedance matching, Opt. Express **15,** 6762 (2007).

[45] E. J. Dias and F. J. García De Abajo, Fundamental limits to the coupling between light and 2D polaritons by small scatterers, ACS Nano **13,** 5184 (2019).

[46] I. V. Zagorodnev, D. A. Rodionov, and A. A. Zabolotnykh, Effect of retardation on the frequency and linewidth of plasma resonances in a two-dimensional disk of electron gas, Phys. Rev. B **103,** 195431 (2021).

[47] Z. Kuang, L. Zhang, and O. D. Miller, Maximal single-frequency electromagnetic response, Optica **7,** 1746 (2020).

[48] O. D. Miller, O. Ilic, T. Christensen, M. T. H. Reid, H. A. Atwater, J. D. Joannopoulos, M. Soljačić, and S. G. Johnson, Limits to the optical response of graphene and two-dimensional materials, Nano Lett. **17,** 5408 (2017).

[49] For GaAs quantum well with $m^* = 0.067m_0$ this inductance corresponds to sheet density $n_s = 1.2 \times 10^{13}$ cm^{-2}, while $\tau = 0.1$ ps corresponds to mobility $\mu \approx 2600$ cm^2/V s.

[50] V. M. Muravev, I. V. Andreev, S. I. Gubarev, V. N. Belyanin, and I. V. Kukushkin, Fine structure of cyclotron resonance in a two-dimensional electron system, Phys. Rev. B **93,** 041110 (2016).

[51] V. M. Muravev, P. A. Gusikhin, I. V. Andreev, and I. V. Kukushkin, Novel Relativistic Plasma Excitations in a Gated Two-Dimensional Electron System, Phys. Rev. Lett. **114,** 106805 (2015).

[52] V. M. Muravev, P. A. Gusikhin, A. M. Zarezin, A. A. Zabolotnykh, V. A. Volkov, and I. V. Kukushkin, Physical

origin of relativistic plasmons in a two-dimensional electron system, Phys. Rev. B **102**, 81301 (2020).

[53] V. M. Muravev, N. D. Semenov, I. V. Andreev, P. A. Gusikhin, and I. V. Kukushkin, A tunable plasmonic resonator using kinetic 2D inductance and patch capacitance, Appl. Phys. Lett. **117**, 151103 (2020).

[54] J. Costantine, Y. Tawk, S. E. Barbin, and C. G. Christodoulou, Reconfigurable antennas: Design and applications, Proc. IEEE **103**, 424 (2015).

[55] D. Psychogiou, R. Gómez-García, and D. Peroulis, in *2018 IEEE Radio and Wireless Symposium (RWS)* (2018), p. 213.

[56] S. Mikhailov, Plasma instability and amplification of electromagnetic waves in low-dimensional electron systems, Phys. Rev. B **58**, 1517 (1998).

[57] T. Echtermeyer, L. Britnell, P. Jasnos, A. Lombardo, R. Gorbachev, A. Grigorenko, A. Geim, A. Ferrari, and K. Novoselov, Strong plasmonic enhancement of photovoltage in graphene, Nat. Commun. **2**, 458 (2011).

[58] D. Wang, A. E. L. Allcca, T.-F. Chung, A. V. Kildishev, Y. P. Chen, A. Boltasseva, and V. M. Shalaev, Enhancing the graphene photocurrent using surface plasmons and a p-n junction, Light: Sci. Appl. **9**, 126 (2020).